Carcinogenesis vol.33 no.8 pp.1487–1493, 2012
doi:10.1093/carcin/bgs177
Advance Access Publication May 18, 2012

Single-CpG-resolution methylome analysis identifies clinicopathologically aggressive CpG island methylator phenotype clear cell renal cell carcinomas

Eri Arai[1], Suenori Chiku[2], Taisuke Mori[1], Masahiro Gotoh[1], Tohru Nakagawa[3], Hiroyuki Fujimoto[3] and Yae Kanai[1,*]

[1]Division of Molecular Pathology, National Cancer Center Research Institute, Tokyo 104-0045, Japan, [2]Science Solutions Division, Mizuho Information and Research Institute, Inc., Tokyo 101-8443, Japan and [3]Department of Urology, National Cancer Center Hospital, Tokyo 104-0045, Japan

*To whom correspondence should be addressed. Tel: +81 3 3542 2511; Fax: +81 3 3248 2463;
Email: ykanai@ncc.go.jp

To clarify the significance of DNA methylation alterations during renal carcinogenesis, methylome analysis using single-CpG-resolution Infinium array was performed on 29 normal renal cortex tissue (C) samples, 107 non-cancerous renal cortex tissue (N) samples obtained from patients with clear cell renal cell carcinomas (RCCs) and 109 tumorous tissue (T) samples. DNA methylation levels at 4830 CpG sites were already altered in N samples compared with C samples. Unsupervised hierarchical clustering analysis based on DNA methylation levels at the 801 CpG sites, where DNA methylation alterations had occurred in N samples and were inherited by and strengthened in T samples, clustered clear cell RCCs into Cluster A (n = 90) and Cluster B (n = 14). Clinicopathologically aggressive tumors were accumulated in Cluster B, and the cancer-free and overall survival rates of patients in this cluster were significantly lower than those of patients in Cluster A. Clear cell RCCs in Cluster B were characterized by accumulation of DNA hypermethylation on CpG islands and considered to be CpG island methylator phenotype (CIMP)-positive cancers. DNA hypermethylation of the CpG sites on the FAM150A, GRM6, ZNF540, ZFP42, ZNF154, RIMS4, PCDHAC1, KHDRBS2, ASCL2, KCNQ1, PRAC, WNT3A, TRH, FAM78A, ZNF671, SLC13A5 and NKX6-2 genes became hallmarks of CIMP in RCCs. On the other hand, Cluster A was characterized by genome-wide DNA hypomethylation. These data indicated that DNA methylation alterations at precancerous stages may determine tumor aggressiveness and patient outcome. Accumulation of DNA hypermethylation on CpG islands and genome-wide DNA hypomethylation may each underlie distinct pathways of renal carcinogenesis.

Introduction

Clear cell renal cell carcinoma (RCC) is the most common histological subtype of adult kidney cancer and frequently affects working-age adults in midlife. In general, RCCs at an early stage are curable by nephrectomy. However, some RCCs relapse and metastasize to distant organs, even if the resection has been considered complete (1). Such clinicopathological diversity may be attributable to distinct pathways of renal carcinogenesis (2). It is well known that clear cell RCCs are characterized by inactivation of the Von Hippel–Lindau tumor-suppressor gene (3). In addition, systematic resequencing and exome analysis of RCCs are now being performed by The Cancer Genome Atlas (4), The Cancer Genome Project (5) and other international efforts (6). Such efforts have revealed that renal carcinogenesis involves inactivation of histone-modifying genes, such as SETD2 (7), a histone H3 lysine 36 methyltransferase, JARIDIC (KDM5C (7)), a histone H3 lysine 4 demethylase, and UTX (KMD6A (8)), a histone H3 lysine 27 demethylase, as well as the SWI/SNF chromatin-remodeling complex gene, PBRM1 (9). Non-synonymous mutations of the NF2 gene and truncating mutations of the MLL2 gene have also been reported (7). However, such gene mutations cannot fully explain the clinicopathological diversity of clear cell RCCs.

Not only genetic, but also epigenetic events appear to accumulate during carcinogenesis, and both types of event reflect the clinicopathological diversity of cancers in various organs in association with each other (10–12). DNA methylation alterations are one of the most consistent epigenetic changes in human cancers (13–16). In fact, on the basis of methylation-specific PCR (MSP), combined bisulfite restriction enzyme analysis (17,18) and bacterial artificial chromosome array-based methylated CpG island amplification (BAMCA (19,20)), we have suggested that non-cancerous renal cortex tissue obtained from patients with RCCs is already at the precancerous stage associated with DNA methylation alterations, even though no remarkable histological changes are evident and there is no association with chronic inflammation or persistent infection with viruses or other pathogenic microorganisms. Genome-wide analysis using BAMCA revealed that DNA methylation status in non-cancerous renal cortex tissue at the precancerous stage was basically inherited by the corresponding clear cell RCC in individual patients (19). DNA methylation alterations at the precancerous stage may confer further susceptibility to genetic and epigenetic alterations and generate more malignant clear cell RCCs (2,13). However, in our previous studies using BAMCA, the resolution and the number of probes were limited. Therefore, further analysis is needed to clarify the significance of DNA methylation alterations in renal carcinogenesis.

Recently, methylome analysis using the Infinium array has made it possible to interrogate 27 000 highly informative CpG sites at single-CpG resolution (21). In order to clarify the significance of DNA methylation alterations during renal carcinogenesis, we used the Infinium BeadChip system to perform genome-wide DNA methylation analysis of 29 samples of normal renal cortex tissue (C) obtained from patients without any primary renal tumors, 107 samples of non-cancerous renal cortex tissue (N) from patients with clear cell RCCs and 109 samples of tissue from the tumors (T) themselves. Correlations between the genome-wide DNA methylation profiles and clinicopathological parameters were then examined.

Abbreviations: BAMCA, bacterial artificial chromosome array-based methylated CpG island amplification; C, normal renal cortex tissue obtained from patients without any primary renal tumor; CIMP, CpG island methylator phenotype; HCC, hepatocellular carcinoma; N, non-cancerous renal cortex tissue obtained from patients with clear cell renal cell carcinomas; NCBI, National Center for Biotechnology Information; RCC, renal cell carcinoma; T, tumorous tissue; TNM, Tumor-Node-Metastasis.

Materials and methods

Patients and tissue samples

The 109 T samples and corresponding 107 N samples showing no remarkable histological changes were obtained from materials that had been surgically resected from 110 patients with primary clear cell RCCs. These patients did not receive preoperative treatment and underwent nephrectomy at the National Cancer Center Hospital, Tokyo, Japan. There were 79 men and 31 women with a mean (±SD) age of 62.8 ± 10.3 years (range 36–85 years). Histological diagnosis was made in accordance with the World Health Organization classification (22) (Supplementary Figure S1, available at *Carcinogenesis* Online). All the tumors were graded on the basis of criteria described previously (23) and classified according to the pathological Tumor-Node-Metastasis (TNM) classification (24). The criteria for macroscopic configuration of RCC (17–19) followed those established for hepatocellular carcinoma (HCC): type 3 (contiguous multinodular type) HCCs show poorer histological differentiation and a higher incidence of intrahepatic metastasis than type 1 (single nodular type) and type 2 (single nodular type with extranodular growth) HCCs (25). The presence or absence of vascular involvement was examined microscopically on slides stained with hematoxylin–eosin and elastica van Gieson. The presence or absence of tumor thrombi in the main trunk of the renal vein was examined macroscopically.

RCC is usually enclosed by a fibrous capsule and well demarcated, and hardly ever contains fibrous stroma between cancer cells. Therefore, we were able to obtain cancer cells from surgical specimens, avoiding contamination with both non-cancerous epithelial cells and stromal cells.

For comparison, 29 samples of normal renal cortex tissue (C1–C29) were obtained from materials that had been surgically resected from 29 patients without any primary renal tumor. These patients included 18 men and 11 women with a mean (±SD) age of 61.4±10.8 years (range 31–81 years). Of these patients, 22 had undergone nephroureterectomy for urothelial carcinomas of the renal pelvis and ureter, 6 had undergone nephrectomy with resection of retroperitoneal sarcoma around the kidney, and the remaining 1 had undergone paraaortic lymph node dissection for metastatic germ cell tumor, which resulted in simultaneous nephrectomy because it was not possible to preserve the renal artery.

All patients included in this study provided written informed consent, and the study was approved by the Ethics Committee of the National Cancer Center, Tokyo, Japan.

Infinium assay

High-molecular-weight DNA from fresh frozen tissue samples was extracted using phenol–chloroform, followed by dialysis (26). Five-hundred-nanogram aliquots of DNA were subjected to bisulfite conversion using an EZ DNA Methylation-Gold™ Kit (Zymo Research, Irvine, CA). Subsequently DNA methylation status at 27 578 CpG loci was examined at single-CpG resolution using the Infinium HumanMethylation27 Bead Array (Illumina, San Diego, CA). This array contains CpG sites located within the proximal promoter regions of the transcription start sites of 14 475 consensus coding sequences in the National Center for Biotechnology Information Database. On average, two assays were selected per gene, and from 3 to 20 CpG sites for more than 200 cancer-related and imprinted genes. Forty control probes were employed for each array; these included staining, hybridization, extension, bisulfite conversion and negative controls. An Evo robot (Tecan, Switzerland) was used for automated sample processing. Whole-genome amplification was performed using the Infinium Assay Kit (Illumina (21)). After hybridization, the specifically hybridized DNA was fluorescence labeled by a single-base extension reaction and detected using a BeadScan reader (Illumina) in accordance with the manufacturer's protocols. The data were then assembled using GenomeStudio methylation software (Illumina). At each CpG site, the ratio of the fluorescent signal was measured using a methylated probe relative to the sum of the methylated and unmethylated probes, i.e. the so-called β-value, which ranges from 0.00 to 1.00, reflecting the methylation level of an individual CpG site.

Statistics

In the Infinium assay, the call proportions (*P*-values for detection of signals above the background <0.01) for 32 probes (shown in Supplementary Table S1, available at *Carcinogenesis* Online) in all of the tissue samples examined were less than 90%. Since such a low proportion may be attributable to polymorphism at the probe CpG sites, these 32 probes were excluded from the present assay. In addition, all CpG sites on chromosomes X and Y were excluded, to avoid any gender-specific methylation bias, leaving a final total of 26 454 autosomal CpG sites.

Infinium probes showing significant differences in DNA methylation levels between the 29 C and 107 N samples were identified by a logistic model adjusted by sex, age and experimental batch. Ordered differences from 29 C to 107 N and then to 109 T samples themselves were examined by the cumulative logit model adjusted by sex, age and experimental batch. Differences of DNA methylation status between 104 paired samples of N and the corresponding T obtained from a single patient and assayed in the same experimental batch were examined by Wilcoxon matched pairs test. A false discovery rate (FDR) of $q = 0.01$ was considered significant. Unsupervised hierarchical clustering (Euclidan distance, Ward method) based on DNA methylation levels ($\Delta\beta_{T-N}$) was performed in patients with clear cell RCCs. Correlations between clusters of patients and clinicopathological parameters were examined using Wilcoxon rank sum test and Fisher's exact test. Survival curves of patients belonging to each cluster were calculated by the Kaplan–Meier method, and the differences were compared by the log-rank test. The number of Infinium assay probes showing DNA hyper- or hypomethylation in each cluster and the average DNA methylation levels ($\Delta\beta_{T-N}$) of each cluster were examined using Wilcoxon rank sum test at a significance level of $P < 0.05$. The CpG sites discriminating the clusters were identified by Fisher's exact test and random forest analysis (27).

Results

DNA methylation alterations during renal carcinogenesis

First, DNA methylation levels of representative CpG sites based on the Infinium assay were clearly verified using a highly quantitative pyrosequencing method (Supplementary Figure S2, available at *Carcinogenesis* Online). With regard to the well-known methylation-silencing Von Hippel–Lindau tumor-suppressor gene (probe Target ID: cg22782492), DNA hypermethylation ($\Delta\beta_{T-N} > 0.1$) was detected in 12 (12%) of 104 patients, for whom both N and T samples were assayed in the same experimental batch. This incidence corresponded to that in previous reports (28,29). Taken together, the data confirmed the reliability of the present Infinium assay.

Although precancerous conditions in the kidney have been rarely described, our previous study suggested that N samples are already at precancerous stages, from the viewpoint of altered DNA methylation, despite the absence of any remarkable histological changes and the lack of association with chronic inflammation and persistent infection with viruses or other pathogenic microorganisms (17–20). (a) In fact, the logistic model adjusted by sex, age and experimental batch revealed that DNA methylation levels on 4830 probes were already altered in N samples compared with those in C samples (FDR, $q = 0.01$, Table I). (b) In order to reveal DNA methylation alterations inherited by clear cell RCCs themselves, ordered differences of DNA methylation level from C to N and then to T samples were examined by the cumulative logit model adjusted by sex, age and experimental batch. Ordered differences from C to N and then to T samples were observed on 11 089 probes (FDR, $q = 0.01$, Table I). (c) In order to reveal the cancer-prone DNA methylation alterations, differences in DNA methylation levels between 104 paired samples of N and T assayed in the same experimental batch were examined using the Wilcoxon matched pairs test. Significant differences between N and the corresponding clear cell RCCs themselves were observed on 10 870 probes (FDR, $q = 0.01$, Table I).

DNA hypermethylation frequently occurred at the very early stages of renal carcinogenesis [(a) in Table I], whereas DNA hypomethylation was also observed during progression to established cancers [(b) and (c) in Table I]. Eight hundred and one probes satisfied all of the above criteria (a)–(c) (Table I): DNA methylation alterations on these 801 probes (Supplementary Table S2, available at *Carcinogenesis* Online) were already evident in N samples, and were inherited by and strengthened in T samples.

Table I. DNA methylation alterations during renal carcinogenesis

The number of probes showing DNA hypermethylation and DNA hypomethylation	
(a) The probes on which DNA methylation levels were altered in samples of non-cancerous renal cortex tissue (N) obtained from patients with clear cell RCCs relative to those in samples of normal renal cortex tissue (C) obtained from patients without any primary renal tumor. (Logistic model adjusted by sex, age and experimental batch; FDR, $q = 0.01$.)	
DNA hypermethylation ($\beta_N > \beta_C$)	4589[a]
DNA hypomethylation ($\beta_N < \beta_C$)	241[b]
Total	4830
(b) The probes on which DNA methylation levels showed ordered differences from C to N, and then to tumorous tissue (T) samples. (Cumulative logit model adjusted by sex, age and experimental batch; FDR, $q = 0.01$.)	
DNA hypermethylation ($\beta_C < \beta_N < \beta_T$, $\beta_C < \beta_N \fallingdotseq \beta_T$ or $\beta_C \fallingdotseq \beta_N < \beta_T$)	6653
DNA hypomethylation ($\beta_C > \beta_N > \beta_T$, $\beta_C > \beta_N \fallingdotseq \beta_T$ or $\beta_C \fallingdotseq \beta_N > \beta_T$)	4436
Total	11 089
(c) The probes on which DNA methylation levels differed between T and the corresponding N samples (Wilcoxon matched pairs test; FDR, $q = 0.01$)	
DNA hypermethylation ($\Delta\beta_{T-N} > 0$)	5408
DNA hypomethylation ($\Delta\beta_{T-N} < 0$)	5462
Total	10 870

[a]Among the 4589 probes, 2675 showed DNA hypermethylation in T samples than in C samples ($\beta_T > \beta_C$; FDR, $q = 0.01$).
[b]Among the 241 probes, 126 showed DNA hypomethylation in T samples than in C samples ($\beta_T < \beta_C$; FDR, $q = 0.01$).

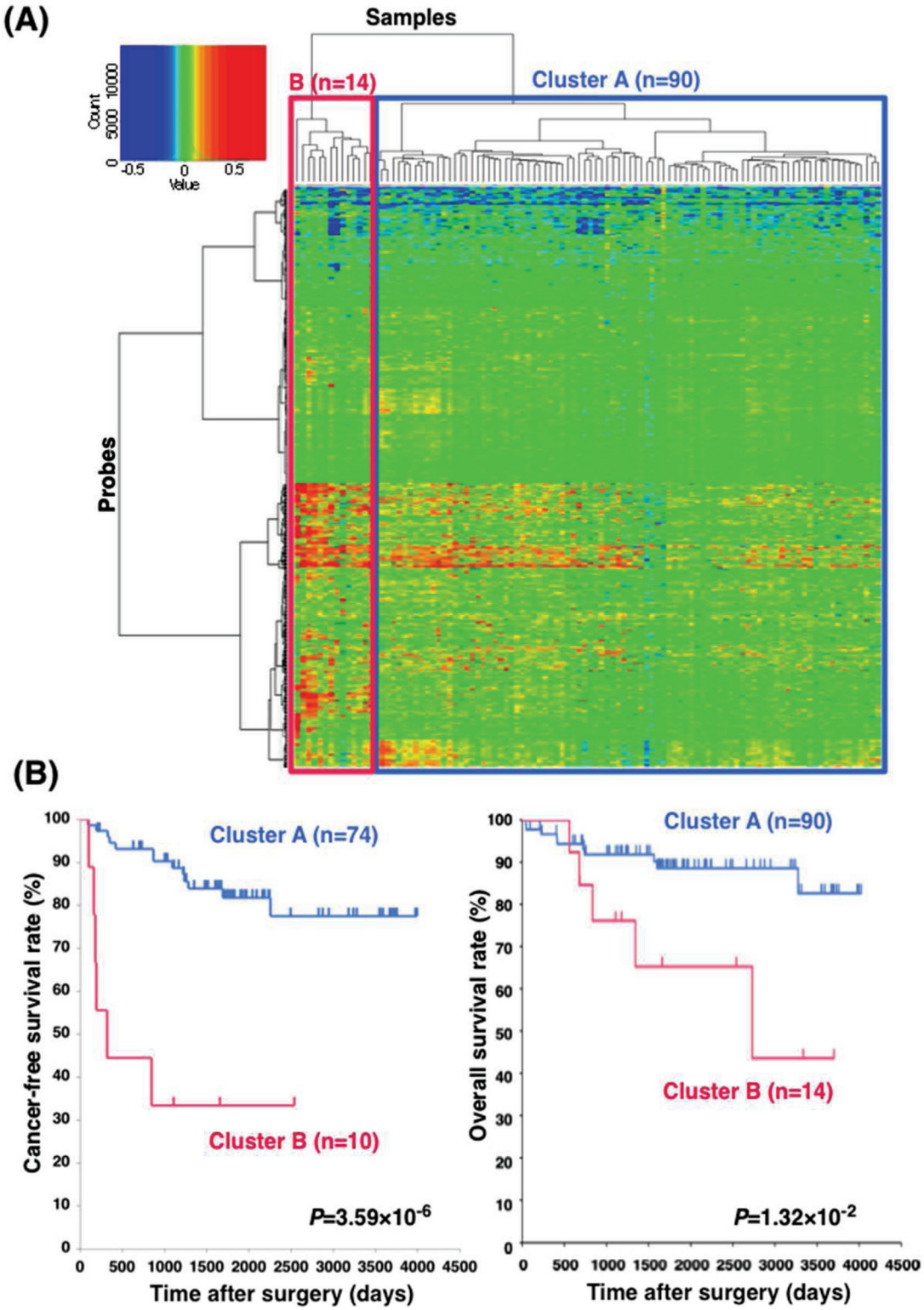

Fig. 1. Unsupervised hierarchical clustering using DNA methylation levels ($\Delta\beta_{T-N}$) on the 801 probes in 104 patients with clear cell RCCs. The 801 probes satisfied all of the criteria (a), (b) and (c) in 'DNA methylation alterations during renal carcinogenesis' in Results and Table I. On the 801 probes, DNA methylation alterations occurred at the precancerous stages and were inherited by and strengthened in clear cell RCCs themselves. (**A**) 104 patients with clear cell RCCs were hierarchically clustered into Cluster A ($n = 90$) and Cluster B ($n = 14$). The DNA methylation levels ($\Delta\beta_{T-N}$) are shown in the color range maps. The cluster trees for patients and probes are shown at the top and left of the panel, respectively. (**B**) The cancer-free ($P = 3.59 \times 10^{-6}$) survival rates of Stage I–III patients in Cluster B were significantly lower (log-rank test) than those of patients in Cluster A. Overall ($P = 1.32 \times 10^{-2}$) survival rates of all patients in Cluster B were significantly lower (log-rank test) than those of patients in Cluster A.

Epigenetic clustering of clear cell RCCs

Unsupervised hierarchical clustering using DNA methylation levels ($\Delta\beta_{T-N}$) on the above 801 probes, on which DNA methylation alterations occurred at the precancerous stages and may continuously participate in renal carcinogenesis, subclustered 104 patients with clear cell RCCs, of whom both N and T samples were assayed in the same experimental batch, into Cluster A (n = 90) and Cluster B (n = 14, Figure 1A). The clinicopathological parameters of clear cell RCCs belonging to Clusters A and B are summarized in Table II. (The number of samples for each TNM stage is also described in Supplementary Table S3, available at *Carcinogenesis* Online.) Epigenetic clustering of clear cell RCCs was dependent on neither age nor sex of the patients (Table II). Clear cell RCCs belonging to Cluster B had a larger diameter, more frequent macroscopically evident extranodular (type 2) or multinodular (type 3) growth, vascular involvement, renal vein tumor thrombi, infiltrating growth, tumor necrosis and renal pelvis invasion, and also had higher histological grades and pathological TNM stages than those in Cluster A (Table II). Figure 1B shows the Kaplan–Meier survival curves of patients belonging to Clusters A and B. The period covered ranged from 42 to 4024 days (mean, 1821 days). The cancer-free and overall survival rates of patients in Cluster B were significantly lower than those of patients in Cluster A ($P = 3.59 \times 10^{-6}$ and $P = 1.32 \times 10^{-2}$, respectively, Figure 1B).

Table II. Correlation between the subclassification of patients with clear cell RRCs based on DNA methylation profiles and the clinicopathological parameters

Clinicopathological parameters		Cluster A (n = 90)	Cluster B (n = 14)	P [a]
Age		62.08 ± 10.08	67.36 ± 11.06	8.36×10^{-2} [b]
Sex	Male	63	11	5.47×10^{-1} [c]
	Female	27	3	
Tumor diameter (cm)		5.10 ± 3.19	8.75 ± 2.85	*1.07×10^{-4}* [b]
Macroscopic configuration	Type 1	37	1	*6.29×10^{-4}* [c]
	Type 2	29	2	
	Type 3	24	11	
Predominant histological grades[d]	G1	47	1	*8.33×10^{-6}* [c]
	G2	35	4	
	G3	7	7	
	G4	1	2	
Highest histological grades[e]	G1	8	0	*5.67×10^{-4}* [c]
	G2	43	1	
	G3	24	4	
	G4	15	9	
Vascular involvement	Negative	54	1	*2.45×10^{-4}* [c]
	Positive	36	13	
Renal vein tumor thrombi	Negative	69	5	*3.38×10^{-3}* [c]
	Positive	21	9	
Predominant growth pattern[d]	Expansive	84	7	*1.86×10^{-4}* [c]
	Infiltrative	6	7	
Most aggressive growth pattern[e]	Expansive	57	4	*2.06×10^{-3}* [c]
	Infiltrative	33	10	
Tumor necrosis	Negative	71	2	*4.86×10^{-6}* [c]
	Positive	19	12	
Invasion to renal pelvis	Negative	83	10	*3.98×10^{-2}* [c]
	Positive	7	4	
Pathological TNM stage	Stage I	50	0	*5.41×10^{-5}* [c]
	Stage II	1	1	
	Stage III	23	9	
	Stage IV	16	4	

The number of samples in each TNM stage was described in Supplementary Table S3, available at *Carcinogenesis* Online.
[a]*P*-values of <0.05 are in italics.
[b]Wilcoxon rank sum test.
[c]Fisher's exact test.
[d]If the tumor showed heterogeneity, findings in the predominant area were described.
[e]If the tumor showed heterogeneity, the most aggressive features of the tumor were described.

DNA methylation profiles of clear cell RCCs belonging to each cluster

The distribution of DNA methylation levels ($\Delta\beta_{T-N}$) in all 26 454 probes for 104 clear cell RCCs belonging to Cluster A or B is summarized along chromosomes in Figure 2A. Clear cell RCCs belonging to Cluster B clearly showed accumulation of DNA hypermethylation ($\Delta\beta_{T-N} > 0.1$) relative to DNA hypomethylation, whereas clear cell RCCs belonging to Cluster A showed greater DNA hypomethylation ($\Delta\beta_{T-N} < -0.1$) relative to DNA hypermethylation (Figure 2A).

The proportions of the probes showing the various degrees of DNA hypermethylation in T samples compared with the corresponding N samples ($\Delta\beta_{T-N} > 0.1$, 0.2, 0.3, 0.4 or 0.5) for all 26 454 probes, and the proportions of the probes showing various degrees of DNA hypomethylation in T samples compared with the corresponding N samples ($\Delta\beta_{T-N} < -0.1$, −0.2, −0.3, −0.4 or −0.5) for all 26 454 probes in clear cell RCCs belonging to Clusters A and B are summarized in Figure 2B. Although the probes showing prominent DNA hypomethylation ($\Delta\beta_{T-N} < -0.5$) were accumulated slightly more in Cluster B than in Cluster A, the incidence of DNA hypomethylation in Clusters A and B did not reach a statistically significant difference ($\Delta\beta_{T-N} < -0.1$, −0.2, −0.3 or −0.4, Figure 2B). On the other hand, the probes showing DNA hypermethylation were markedly accumulated in Cluster B relative to Cluster A, regardless of the degree of DNA hypermethylation ($\Delta\beta_{T-N} > 0.1$, 0.2, 0.3, 0.4 or 0.5, Figure 2B). These data indicate that clear cell RCCs belonging to Cluster B are characterized by accumulation of DNA hypermethylation.

The top 61 probes (including the 60th and 61st, which showed equivalent P-values) on which DNA methylation levels ($\Delta\beta_{T-N}$) differed markedly between Clusters A and B ($P < 1.056 \times 10^{-6}$, Wilcoxon rank sum test) are listed in Supplementary Table S4, available at *Carcinogenesis* Online. Although only 19 246 probes (72.8%) out of the total of 26 454 were located within CpG islands, 60 (98.4%) of the top 61 probes located within CpG islands showed DNA hypermethylation in clear cell RCCs belonging to Cluster B ($\Delta\beta_{T-N} > 0.097$, Supplementary Table S4, available at *Carcinogenesis* Online): only 1 probe among the top 61 was located within a non-CpG island and showed DNA hypomethylation ($\Delta\beta_{T-N} = -0.425 \pm 0.096$ in Cluster B). Taken together, the data indicated that Cluster B is significantly correlated with clinicopathological phenotype and characterized by frequent DNA hypermethylation on CpG islands. Such characteristics of clear cell RCCs in Cluster B are similar to those of CpG island methylator phenotype (CIMP)-positive cancers (30,31) in other well-studied organs, such as those of the colon (32) and stomach (33). In other words, our single-CpG-resolution methylome analysis identified, for the first time, CIMP-positive clear cell RCCs as Cluster B.

Hallmark CpG sites of CIMP-positive clear cell RCCs

Scattergrams of DNA methylation levels (β values) in T and the corresponding N samples from representative patients with clear cell RCCs belonging to Clusters A and B (Supplementary Figure S3, available at *Carcinogenesis* Online) indicated that probes for which DNA methylation levels were low in the N samples and for which the degree of DNA hypermethylation in T samples relative to the corresponding N samples was prominent (marked by red circles in panels E to H in Supplementary Figure S3, available at *Carcinogenesis* Online) were obvious only in Cluster B, and not in Cluster A.

Therefore, in order to discriminate clear cell RCCs belonging to Cluster B from those belonging to Cluster A, we first focused on the probes for which the average β value in all N samples was less than 0.2 and the incidence of more than $0.4\Delta\beta_{T-N}$ was markedly higher in Cluster B relative to Cluster A ($P < 1.98 \times 10^{-6}$, Fisher's exact test). Among such probes, 16 (the FAM150A, GRM6, ZNF540, ZFP42, ZNF154, RIMS4, PCDHAC1, KHDRBS2, ASCL2, KCNQ1, PRAC, ZNF154, WNT3A, TRH, FAM78A and ZNF671 genes) showed $>0.4\Delta\beta_{T-N}$ in 6 (42.8%) or more RCCs among the 14 belonging to Cluster B, but only in 2 (2.2%) or fewer RCCs among the 90 belonging to Cluster A (Table IIIA). DNA methylation levels ($\Delta\beta_{T-N}$) on the 16 CpG sites differed completely between Clusters A and B (Supplementary Figure S4, available at *Carcinogenesis* Online). In addition,

random forest analysis (27) (Supplementary Figure S5, available at *Carcinogenesis* Online) using the 869 probes on which DNA methylation levels ($\Delta\beta_{T-N}$) differed significantly between Clusters A and B [FDR (q = 0.01)] identified the top four probes that were able to discriminate Cluster B from Cluster A in Table IIIB. Two probes were shared by Tables IIIA and IIIB. Thus, CpG sites on the 18 probes can be considered as hallmarks of CIMP-positive clear cell RCCs, i.e. clear cell RCCs belonging to Cluster B.

Discussion

Here, we have reported the results of methylome analysis of 245 renal tissue samples at single-CpG resolution. To our knowledge, no study involving Infinium analysis of such a large number of renal tissue samples has been reported to date. We have been focusing on DNA methylation alterations at the precancerous stage: our previous studies using methylation-specific PCR, combined bisulfite restriction enzyme analysis and bacterial artificial chromosome arrays suggested that N samples are already at the precancerous stage associated with DNA methylation alterations (17–20). First, we identified the probes on which DNA methylation status in N samples were significantly altered relative to those in C samples. The single-CpG-resolution analysis revealed that the DNA methylation status of 4830 CpG sites was actually altered at the precancerous stage in comparison to normal renal cortex tissue samples. In addition, it was revealed that alterations at the precancerous stages tended to involve DNA hypermethylation [Table I(a)]. Among the 801 probes we selected, DNA methylation alterations occurred at the precancerous stage and were inherited by, and strengthened in, clear cell RCCs themselves, indicating that DNA methylation alterations on the 801 probes may participate continuously in renal carcinogenesis from the precancerous stage until cancers have become established. The DNA methylation profiles of these 801 probes clustered clear cell RCCs into clinicopathologically valid subclusters: clear cell RCCs belonging to Cluster B showed clinicopathological parameters reflecting tumor aggressiveness, and patients with Cluster B tumors showed a poorer outcome. Quantitative reverse transcription–PCR analysis indicated that DNA hypermethylation may result in significantly reduced expression of representative genes listed in Tables IIIA and IIIB and Supplementary Table S4, available at *Carcinogenesis* Online (Supplementary Table S5, available at *Carcinogenesis* Online). These findings suggest that DNA

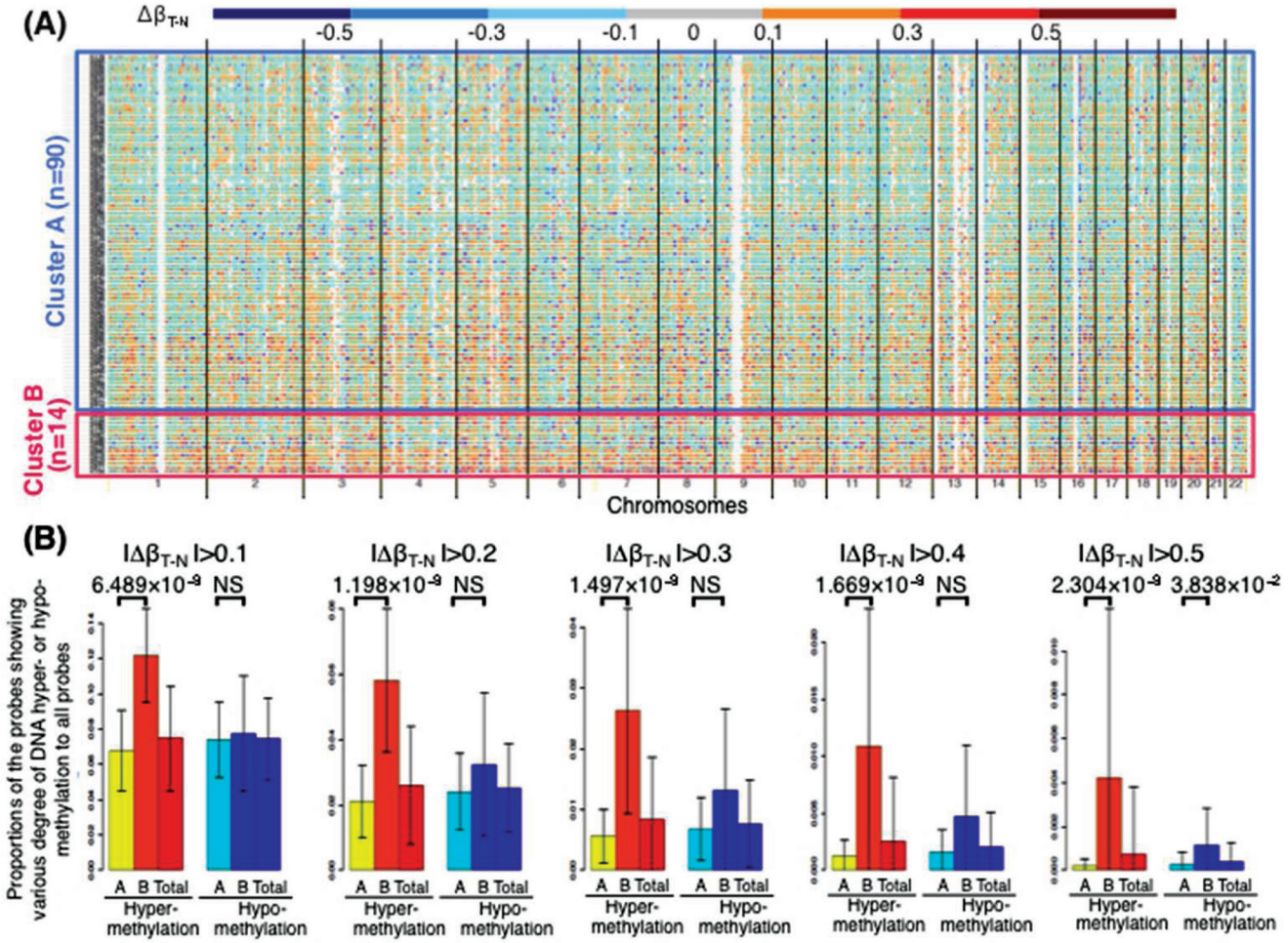

Fig. 2. (**A**) Distribution of DNA methylation levels ($\Delta\beta_{T-N}$) in all 26 454 probes in 104 clear cell RCCs belonging to Cluster A or B. The DNA methylation levels are shown in the color range maps. Clear cell RCCs belonging to Cluster A are skewed toward DNA hypomethylation ($\Delta\beta_{T-N} < -0.1$, cold color) relative to DNA hypermethylation (warm color). Clear cell RCCs belonging to Cluster B clearly showed accumulation of DNA hypermethylation ($\Delta\beta_{T-N} > 0.1$, warm color) relative to DNA hypomethylation (cold color). (**B**) The proportions of the probes showing the various degrees of DNA hypermethylation, when the tumor tissue (T) sample was compared with the corresponding non-cancerous renal cortex tissue (N) sample ($\Delta\beta_{T-N} > 0.1$, 0.2, 0.3, 0.4 or 0.5, warm color), to all probes, and the proportions of the probes showing the various degrees of DNA hypomethylation, when the T sample was compared with the corresponding N sample ($\Delta\beta_{T-N} < -0.1$, −0.2, −0.3, −0.4 or −0.5, cold color), to all probes in Clusters A and B. Bar, standard deviation. The probes showing DNA hypermethylation were markedly accumulated in Cluster B relative to Cluster A, regardless of the degree of DNA hypermethylation ($\Delta\beta_{T-N} > 0.1$, 0.2, 0.3, 0.4 or 0.5). The probes showing prominent DNA hypomethylation ($\Delta\beta_{T-N} < -0.5$) were slightly accumulated in Cluster B compared with Cluster A. These data indicated that clear cell RCCs belonging to Cluster B are mainly characterized by accumulation of DNA hypermethylation.

Table IIIA. CpG sites as hallmarks of the CpG island methylator phenotype of clear cell RRCs

Target ID[a]	Chr[b]	Position[c]	CpG island[d]	Gene symbol	The number of tumors whose $\Delta\beta_{T-N} > 0.4$ (%)[e]		P [f]
					Cluster A (n = 90)	Cluster B (n = 14)	
cg17162024	8	53,478,454	Y	FAM150A	2 (2.2)	12 (85.7)	4.60×10^{-12}
cg14859460	5	178,422,244	Y	GRM6	0 (0)	10 (71.4)	3.84×10^{-11}
cg03975694	19	38,042,472	Y	ZNF540	2 (2.2)	9 (64.3)	3.64×10^{-8}
cg06274159	4	188,916,867	Y	ZFP42	1 (1.1)	8 (57.1)	9.91×10^{-8}
cg08668790	19	58,220,662	Y	ZNF154	1 (1.1)	8 (57.1)	9.91×10^{-8}
cg19332710	20	43,438,865	Y	RIMS4	2 (2.2)	8 (57.1)	4.68×10^{-7}
cg12629325	5	140,306,458	Y	PCDHAC1	2 (2.2)	7 (50)	5.10×10^{-6}
cg18239753	6	62,995,963	Y	KHDRBS2	2 (2.2)	7 (50)	5.10×10^{-6}
cg06263495	11	2,292,004	Y	ASCL2	2 (2.2)	7 (50)	5.10×10^{-6}
cg17575811	11	2,466,409	Y	KCNQ1	1 (1.1)	7 (50)	1.21×10^{-6}
cg12374721	17	46,799,640	Y	PRAC	2 (2.2)	7 (50)	5.10×10^{-6}
cg21790626	19	58,220,494	Y	ZNF154	0 (0)	7 (50)	1.62×10^{-7}
cg01322134	1	228,194,448	Y	WNT3A	0 (0)	6 (42.9)	1.98×10^{-6}
cg01009664	3	129,693,613	Y	TRH	0 (0)	6 (42.9)	1.98×10^{-6}
cg12998491	9	134,152,531	Y	FAM78A	0 (0)	6 (42.9)	1.98×10^{-6}
cg19246110	19	58,238,928	Y	ZNF671	0 (0)	6 (42.9)	1.98×10^{-6}

[a]Probe ID for the Infinium HumanMethylation27 Bead Array.
[b]Chromosome.
[c]National Center for Biotechnology Information (NCBI) Database (Genome Build 37).
[d]Y means CpG island.
The probes satisfied the following criteria: (i) the average β value for all samples of non-cancerous renal cortex tissue (N) was <0.2, (ii) $>0.4\Delta\beta_{T-N}$ was observed in six or more clear cell RCCs (≥42.9%)[e] in Cluster B, whereas $>0.4\Delta\beta_{T-N}$ in two or fewer clear cell RCCs (≤2.2%)[e] in Cluster A and (iii) the incidence of $>0.4\Delta\beta_{T-N}$ was markedly higher in Cluster B than in Cluster A ($P < 1.98 \times 10^{-6}$, Fisher's exact test[f]).

Table IIIB. CpG sites as hallmarks of the CpG island methylator phenotype of clear cell RRCs

Target ID[a]	Chr[b]	Position[c]	CpG island[d]	Gene symbol	$\Delta\beta_{T-N}$ (mean ± SD)		P [e]
					Cluster A (n = 90)	Cluster B (n = 14)	
cg17162024	8	53,478,454	Y	FAM150A[f]	0.126 ± 0.120	0.499 ± 0.184	3.40×10^{-7}
cg22040627	17	6,617,030	Y	SLC13A5	0.045 ± 0.072	0.283 ± 0.103	2.64×10^{-7}
cg14859460	5	178,422,244	Y	GRM6[f]	0.077 ± 0.105	0.434 ± 0.184	1.10×10^{-7}
cg09260089	10	134,599,860	Y	NKX6-2	0.078 ± 0.083	0.372 ± 0.150	2.26×10^{-7}

[a]Probe ID of the Infinium HumanMethylation27 Bead Array.
[b]Chromosome.
[c]NCBI Database (Genome Build 37).
[d]Y means CpG island.
[e]Top four probes capable of discriminating Cluster B from Cluster A identified by random forest analysis (Supplementary Figure S5, available at *Carcinogenesis* Online) using the 869 probes on which the DNA methylation levels ($\Delta\beta_{T-N}$) were differed significantly between Clusters A and B (Wilcoxon rank sum test).
[f]The FAM150A and GRM6 genes were shared by Tables IIIA and IIIB.

methylation alterations occurring at the precancerous stage determine both the aggressiveness of RCCs and the outcome of affected patients through alterations of gene expression levels.

Unsupervised hierarchical clustering based on our previous study using bacterial artificial chromosome arrays also clustered clear cell RCCs into clinicopathologically valid subclusters: 14% of examined RCCs belonged to a subcluster showing clinicopathological parameters reflecting tumor aggressiveness and poorer patient outcome (19). DNA methylation profiles in N samples based on BAMCA data were also inherited by the corresponding clear cell RCC developing in the same patient. In this study, 14% of the clear cell RCCs subjected to Infinium analysis belonged to Cluster B. BAMCA is suitable for detecting DNA methylation alterations occurring in a coordinated manner on individual large regions of chromosomes (34–37), whereas 27 000 Infinium array is suitable for detecting DNA methylation alterations on promoter regions of specific genes. Different methodologies identified similar clinicopathologically valid subclusters of RCCs, indicating that such clustering based on DNA methylation profiles is not accidental but reproducible, and may reflect the distinct epigenetic pathway of renal carcinogenesis.

In contrast to Cluster A, which appeared to be characterized by accumulation of DNA hypomethylation (Figure 2A), Cluster B was clearly characterized by accumulations of DNA hypermethylation on CpG islands. Since Cluster B was significantly associated with both frequent DNA hypermethylation on CpG islands and distinct clinicopathological phenotypes of clear cell RCCs, RCCs belonging to Cluster B can be recognized as CIMP-positive clear cell RCCs on the basis of the definition of well-studied CIMP-positive cancers (30,31) such as colorectal cancer (32) and stomach cancer (33), although Morris *et al*. (28) previously considered that the relevance of the CIMP-positive phenotype to RCCs had not yet been clearly defined. Although McRonald *et al*. (29) suggested that a subset of RCCs might display CIMP based on findings indicating that the distribution of the number of methylated CpGs in individual tumors differed from the expected Poisson distribution, they did not identify distinct CpG sites that could become hallmarks for CIMP in the kidney. It has been suggested that, in order to identify CIMP-positive cancers in specific organs, marker CpG sites or genes that are specific to each organ or histological type of tumor should be used (38), rather than classical CIMP marker genes (30,31) that were originally identified in colorectal cancers. The present single-CpG-resolution analysis identified such hallmark CpG sites for the first time. Using the 18 CpG sites in Tables IIIA and IIIB, CIMP-positive RCCs or RCCs equivalent to those in the present Cluster B could be reproducibly identified. These 18 CpG sites may be useful for further clarifying the molecular basis of the epigenetic pathway of renal carcinogenesis.

DNA methylation alterations are known to result in chromosomal instability through chromatin configuration changes (39). In fact, germline mutations of the de novo DNA methyltransferase DNMT3B gene have been reported in patients with immunodeficiency, centromeric instability and facial anomalies (ICF) syndrome, a rare recessive autosomal disorder characterized by DNA hypomethylation of pericentromeric satellite regions (40). In HCCs and urothelial carcinomas, DNA hypomethylation of these regions is correlated with copy number alterations on chromosomes 1 (41) and 9 (42), respectively, where satellite regions are plentiful. Correlations between the clustering based on Infinium assay and copy number alterations should be further examined.

Taken together, the data suggest that in CIMP-positive clear cell RCCs belonging to Cluster B, DNA hypermethylation of distinct CpG islands participates even in the very early and precancerous stages. Such DNA methylation alterations occurring in the precancerous stages may induce more aggressive tumor phenotypes and poorer patient outcome in Cluster B. On the other hand, in the other pathway of renal carcinogenesis leading to clear cell RCCs in Cluster A, DNA hypomethylation may be a later event (Table I) than DNA hypermethylation on CpG islands. We are now performing exome, transcriptome and proteome analyses of RCCs belonging to both clusters. Such multilayer omics analyses may identify the upstream genetic events inducing DNA methylation profiles and key signal pathways that characterize Clusters A and B.

Supplementary material

Supplementary Figures S1–S5 and Tables S1–S5 can be found at http://carcin.oxfordjournals.org/.

Funding

Program for Promotion of Fundamental Studies in Health Sciences of the National Institute of Biomedical Innovation (NiBio); Grant-in-Aid for the Third Term Comprehensive 10-Year Strategy for Cancer Control from the Ministry of Health, Labor and Welfare of Japan; National Cancer Center Research and Development Fund; Grants-in-Aid for Scientific Research (B) and for Young Scientists (B) from the Japan Society for the Promotion of Science (JSPS).

Acknowledgements

Conflict of Interest Statement: None declared.

References

1. Ljungberg,B. *et al.* (2011) The epidemiology of renal cell carcinoma. *Eur. Urol.*, **60**, 615–621.
2. Arai,E. *et al.* (2011) Genetic and epigenetic alterations during renal carcinogenesis. *Int. J. Clin. Exp. Pathol.*, **4**, 58–73.
3. Baldewijns,M.M. *et al.* (2010) VHL and HIF signalling in renal cell carcinogenesis. *J. Pathol.*, **221**, 125–138.
4. Barrett,I.P. (2010) Cancer genome analysis informatics. *Methods Mol. Biol.*, **628**, 75–102.
5. Zhang,J. *et al.* (2011) International Cancer Genome Consortium Data Portal--a one-stop shop for cancer genomics data. *Database (Oxford)*, **2011**, bar026.
6. Brannon,A.R. *et al.* (2010) Renal cell carcinoma: where will the state-of-the-art lead us? *Curr. Oncol. Rep.*, **12**, 193–201.
7. Dalgliesh,G.L. *et al.* (2010) Systematic sequencing of renal carcinoma reveals inactivation of histone modifying genes. *Nature*, **463**, 360–363.
8. van Haaften,G. *et al.* (2009) Somatic mutations of the histone H3K27 demethylase gene UTX in human cancer. *Nat. Genet.*, **41**, 521–523.
9. Varela,I. *et al.* (2011) Exome sequencing identifies frequent mutation of the SWI/SNF complex gene PBRM1 in renal carcinoma. *Nature*, **469**, 539–542.
10. Baylin,S.B. *et al.* (2011) A decade of exploring the cancer epigenome - biological and translational implications. *Nat. Rev. Cancer*, **11**, 726–734.
11. Boumber,Y. *et al.* (2011) Epigenetics in cancer: what's the future? *Oncology (Williston Park)*, **25**, 220–226, 228.
12. Jones,P.A. *et al.* (2007) The epigenomics of cancer. *Cell*, **128**, 683–692.
13. Kanai,Y. (2010) Genome-wide DNA methylation profiles in precancerous conditions and cancers. *Cancer Sci.*, **101**, 36–45.
14. Arai,E. *et al.* (2010) DNA methylation profiles in precancerous tissue and cancers: carcinogenetic risk estimation and prognostication based on DNA methylation status. *Epigenomics*, **2**, 467–481.
15. Kanai,Y. (2008) Alterations of DNA methylation and clinicopathological diversity of human cancers. *Pathol. Int.*, **58**, 544–558.
16. Kanai,Y. *et al.* (2007) Alterations of DNA methylation associated with abnormalities of DNA methyltransferases in human cancers during transition from a precancerous to a malignant state. *Carcinogenesis*, **28**, 2434–2442.
17. Arai,E. *et al.* (2008) Genetic clustering of clear cell renal cell carcinoma based on array-comparative genomic hybridization: its association with DNA methylation alteration and patient outcome. *Clin. Cancer Res.*, **14**, 5531–5539.
18. Arai,E. *et al.* (2006) Regional DNA hypermethylation and DNA methyltransferase (DNMT) 1 protein overexpression in both renal tumors and corresponding nontumorous renal tissues. *Int. J. Cancer*, **119**, 288–296.
19. Arai,E. *et al.* (2009) Genome-wide DNA methylation profiles in both precancerous conditions and clear cell renal cell carcinomas are correlated with malignant potential and patient outcome. *Carcinogenesis*, **30**, 214–221.
20. Arai,E. *et al.* (2011) Genome-wide DNA methylation profiles in renal tumors of various histological subtypes and non-tumorous renal tissues. *Pathobiology*, **78**, 1–9.
21. Bibikova,M. *et al.* (2009) Genome-wide DNA methylation profiling using Infinium® assay. *Epigenomics*, **1**, 177–200.
22. Eble,J.N. *et al.* (2004) Renal cell carcinoma. *World Health Organization Classification of Tumours. Pathology and Genetics. Tumours of the Urinary System and Male Genital Organs*. IARC Press, Lyon, pp. 10–43.
23. Fuhrman,S.A. *et al.* (1982) Prognostic significance of morphologic parameters in renal cell carcinoma. *Am. J. Surg. Pathol.*, **6**, 655–663.
24. Sobin,L.H. *et al.* (2002) International Union Against Cancer (UICC). *TNM Classification of Malignant Tumors*. 6th edn. Wiley-Liss, New York, pp. 193–195.
25. Kanai,T. *et al.* (1987) Pathology of small hepatocellular carcinoma. A proposal for a new gross classification. *Cancer*, **60**, 810–819.
26. Sambrook,J. *et al.* (2001) *Molecular Cloning: A Laboratory Manual*. 3rd edn. Cold Spring Harbor Laboratory Press, Cold Spring Harbor, NY, pp. 6.14–6.15.
27. Breiman,L. (2001) Random forests. *Mach. Learn.*, **45**, 5–32.
28. Morris,M.R. *et al.* (2010) Epigenetics of renal cell carcinoma: the path towards new diagnostics and therapeutics. *Genome Med.*, **2**, 59.
29. McRonald,F.E. *et al.* (2009) CpG methylation profiling in VHL related and VHL unrelated renal cell carcinoma. *Mol. Cancer*, **8**, 31.
30. Issa,J.P. (2004) CpG island methylator phenotype in cancer. *Nat. Rev. Cancer*, **4**, 988–993.
31. Toyota,M. *et al.* (1999) CpG island methylator phenotype in colorectal cancer. *Proc. Natl. Acad. Sci. U.S.A.*, **96**, 8681–8686.
32. Shen,L., *et al.* (2007) Integrated genetic and epigenetic analysis identifies three different subclasses of colon cancer. *Proc. Natl. Acad. Sci. U.S.A.*, **104**, 18654–18659.
33. Toyota,M. *et al.* (1999) Aberrant methylation in gastric cancer associated with the CpG island methylator phenotype. *Cancer Res.*, **59**, 5438–5442.
34. Nagashio,R. *et al.* (2011) Carcinogenetic risk estimation based on quantification of DNA methylation levels in liver tissue at the precancerous stage. *Int. J. Cancer*, **129**, 1170–1179.
35. Gotoh,M. *et al.* (2011) Diagnosis and prognostication of ductal adenocarcinomas of the pancreas based on genome-wide DNA methylation profiling by bacterial artificial chromosome array-based methylated CpG island amplification. *J. Biomed. Biotechnol.*, **2011**, 780–836.
36. Nishiyama,N. *et al.* (2010) Genome-wide DNA methylation profiles in urothelial carcinomas and urothelia at the precancerous stage. *Cancer Sci.*, **101**, 231–240.
37. Arai,E. *et al.* (2009) Genome-wide DNA methylation profiles in liver tissue at the precancerous stage and in hepatocellular carcinoma. *Int. J. Cancer*, **125**, 2854–2862.
38. Abe,M. *et al.* (2008) Identification of genes targeted by CpG island methylator phenotype in neuroblastomas, and their possible integrative involvement in poor prognosis. *Oncology*, **74**, 50–60.
39. Eden,A. *et al.* (2003) Chromosomal instability and tumors promoted by DNA hypomethylation. *Science*, **300**, 455.
40. Hansen,R.S. *et al.* (1999) The DNMT3B DNA methyltransferase gene is mutated in the ICF immunodeficiency syndrome. *Proc. Natl. Acad. Sci. U.S.A.*, **96**, 14412–14417.
41. Wong,N. *et al.* (2001) Hypomethylation of chromosome 1 heterochromatin DNA correlates with q-arm copy gain in human hepatocellular carcinoma. *Am. J. Pathol.* **59**, 465–471.
42. Nakagawa,T. *et al.* (2005) DNA hypomethylation on pericentromeric satellite regions significantly correlates with loss of heterozygosity on chromosome 9 in urothelial carcinomas. *J. Urol.*, **173**, 243–246.

Received December 11, 2012; revised April 17, 2012; accepted May 11, 2012